Proceedings of the 9th International Conference on Physical Modelling in Coastal Engineering (Coastlab24)

Delft, Netherlands, May 13-16, 2024

Conference Paper, DOI: 10.59490/coastlab.2024.705

ADCP SUSPENDED SEDIMENT TRANSPORT MONITORING USING ACOUSTIC PARTICLE RADIUS

R.A.J. JAARSMA[1,2], M. DAUGHARTY[1], S.D. KAMMINGA[1], M.A. VAN DER LUGT[2,3], M.A. DE SCHIPPER[2], S. NYLUND[3]

1 Nortek Netherlands B.V., The Netherlands, ruurd.jaarsma@nortekgroup.com, maeve.daugharty@nortekgroup.com

2 Delft University of Technology, The Netherlands

3 Deltares, The Netherlands

4 Nortek AS, Rud, Norway

ABSTRACT

Monitoring suspended sediment concentration (SSC) can be challenging as direct sampling methods are labour intensive and indirect measurements based on optical or acoustic backscatter are sensitive to changes in particle properties. Regardless, using ADCP backscatter to predict SSC is promising because of the possibility to capture suspended sediment transport by combining with flow measurements. To reduce sensitivity of established backscatter-SSC relations to changing particle size, a methodology is proposed where acoustic particle radius is derived using multi-frequency backscatter measurements obtained with a Nortek Signature1000 ADCP equipped with a vertical beam echosounder. Considering acoustic particle radii in an adapted backscatter-SSC model shows promising improvement in correlations with water sample reference measurements compared to the traditional single frequency approach based on a field test. Follow-up assessment is required to overcome limitations in dataset sample size and to investigate further improvements of the method. Still, application of the method can significantly enhance capability of ADCPs predicting SSC and – since backscatter is recorded over depth in conjunction with flow measurements – the ability to monitor suspended sediment transport using a single instrument.

KEYWORDS: Sediment, SSC, Monitoring, ADCP, Backscatter

1 INTRODUCTION

Quantifying suspended sediment transport has been key in various coastal and river engineering projects, for example to study sediment budgets in estuaries or mitigating the impact of dredging activities. As numerical models become more important in understanding and predicting sediment transport phenomena, accurate direct measurements of hydrodynamics and suspended sediment concentration (SSC) will become increasingly crucial for calibration and validation.

Compared to hydrodynamic parameters such as currents and waves, which can be measured directly using a range of in situ instruments, quantifying SSC typically involves a more elaborate process due to limitations in available monitoring methods. Traditional methods such as water sampling are labour intensive and expensive, leading to low temporal and spatial resolutions. Indirect measurements can be based on optical backscatter (OBS), acoustic backscatter (ABS) or laser diffraction, of which OBS point measurement sensors are most widely used to determine SSC due to its well-documented procedure.

Using Acoustic Doppler Current Profilers (ADCPs) – which record ABS as a by-product to the flow velocity signal – to capture suspended sediment structures over depth has been investigated for over three decades (e.g. Reichel & Nachtnebel, 1994; Gartner, 2004; Nauw et al., 2014). If a proper relation between SSC and ADCP backscatter can be established, it is possible to monitor suspended sediment *transport* over the water column by combining the backscatter data with the flow velocity profiles measured by the instrument. This can then be done in vessel-mounted setups, to capture vast spatial resolutions (i.e. transects of tidal inlets) or in stationary buoy or bottom frame setups for long periods of time thanks to the limited vulnerability to biofouling.

Because sensors based on OBS or ABS including ADCPs do not measure SSC directly, but rather record a backscatter intensity ([V], [NTU], [counts], or [dB]) within a sampling volume, a model – referred to as data calibration – must be set up between the measured signal and reference measurements of SSC in [mg/L]. Because SSC and the particle size of the sediment can vary significantly over time, for example with the tidal phase (Plancke et al. 2017), the process of the conversion between

SSC and backscatter intensity can become labour intensive to execute and analyse. Therefore, if this dependency on reference measurements can be reduced, the potential of ADCPs as sediment transport monitoring tool can be significantly enhanced.

To this end, methods to derive information about particle size using multiple acoustic frequencies have been researched (e.g. Topping et al., 2007; Guerrero et al., 2012, 2013; Jourdin et al., 2014). Not only does this potentially provide valuable water column information about sediment class, these estimates can also make the relation between backscatter and SSC more robust, therefore reducing the need for frequently obtaining (water sample) reference measurements. In these earlier studies, obtaining ADCP backscatter profiles at different frequencies required the use of multiple instruments, inevitably leading to alignment issues (Guerrero et al., 2013; Jourdin et al., 2014). To overcome these limitations, a Nortek Signature1000 ADCP was adapted to record near simultaneous and colocated backscatter profiles at multiple frequencies using its vertical beam *echosounder* transducer dedicated for high resolution backscatter measurements. Based on these measurements, particle radius estimates were derived and used to establish an adapted model between backscatter and reference SSC measurements, to assess whether certainty in monitoring suspended sediment concentration and subsequently sediment *transport* using ADCPs can be improved using this instrument.

2 DATA CALIBRATION: DERIVING SSC FROM ADCP BACKSCATTER

2.1 Volume backscatter and signal losses

Traditionally, ADCPs record backscatter intensity (R_x; [dB]) as a signal strength validation parameter for current measurements and is stored in cells over the depth profile. To use ABS as a source of information about suspended sediment particles and compare measurements over depth, the signal must be processed to account for signal losses that vary with distance from the transducer (R), while considering instrument properties and settings, and removing data below the acoustic noise threshold (NT). This can be done using ADCP processing software (Nortek, 2023; Ocean Illumination, 2021) based on the sonar equation:

$$S_v = 10\log_{10}\left(10^{\frac{R_x}{10}} - 10^{\frac{NT}{10}}\right) + 20\log_{10}(R) + 2\alpha R - 10\log_{10}\left(\frac{c\tau}{2}\right) - 10\log_{10}\left(\frac{5.78}{k^2 r^2}\right) - PL + G \quad (1)$$

Here, S_v represents *volume backscatter*, which is the contribution of the ensonified cloud of particles normalized over a theoretical measurement volume of 1 m^3 (*Acoustics Unpacked*, n.d.). Relevant instrument parameters include transducer radius r [m], the applied power level PL [dB], transmit pulse length τ [s], and the acoustic wavenumber k [-]. k depends on the acoustic frequency F [Hz] through $k = \frac{2\pi(1000 \cdot F)}{c}$; where c is the speed of sound through water [m/s]. If measurements are to be compared between instruments, the instrument gain parameter G must be determined following a lab calibration procedure where targets of known backscattering strength are lowered into the acoustic beam of the transducer (Demer et al., 2015; Nortek, 2022). Without instrument calibration, measurements of volume backscatter are relative – indicated with S_v' in this research.

In Equation 1, α is the attenuation coefficient [dB/m], which accounts for signal losses caused by 1) absorption by water (Ainslie & McColm, 1998), and 2) absorption by and scattering losses due to suspended particles. Determining the contribution of the latter requires information about the particles like concentration and size (Guerrero et al., 2016; Thorne & Meral, 2008; Urick, 1948). Methodologies have been developed for estimating attenuation losses due to suspended sediment (e.g. Guerrero & Di Federico, 2018; Sassi et al., 2012), however if concentrations are low enough, the contribution of sediment attenuation to α can be neglected (Gartner, 2004; Hay & Sheng, 1992).

2.2 Backscatter-SSC model

To understand the relation between volume backscatter and suspended sediment parameters such as concentration, size, shape, and density, a general backscatter-SSC model is described here (Sassi et al., 2012). For spherical particles, the concentration of the particles in the water volume (SSC) can be modelled based on the mean particle radius $\langle a_s \rangle$, density ρ_s, and n_b, the number of scattering particles per unit volume:

$$SSC = \frac{4}{3}\pi\rho_s n_b \langle a_s^3 \rangle \quad (2)$$

The terms written in $\langle \cdot \rangle$ denote mean values of backscattering particle characteristics within the ensonified volume. The backscatter from the water volume is related to the mean particle radius within this volume via:

$$S_v = 10\log_{10}\left(n_b \frac{1}{4}\langle a_s^2 f^2 \rangle\right) \quad (3)$$

(Medwin & Clay, 1998, Sassi et al., 2012). Here, f is the so-called form function, and describes the backscattering behaviour of the particles based on the product of the acoustic wavenumber and particle radius ka_s (Thorne & Meral, 2008). For quartz sand particles this form function is expressed by Thorne & Meral (2008):

$$f(a_s) = \frac{(ka_s)^2\left(1-0.35e^{-\left(\frac{ka_s-1.5}{0.7}\right)^2}\right)\left(1+0.5e^{-\left(\frac{ka_s-1.8}{2.2}\right)^2}\right)}{1+0.9(ka_s)^2} \quad (4)$$

Combining Equations 2 and 3 yields a relation between S_v and SSC (Sassi et al., 2012):

$$S_v = 10\log_{10}\left(\frac{\langle a_s^2 f^2\rangle}{\langle a_s^3\rangle}\frac{3}{16\pi\rho_s}SSC\right) \quad (5)$$

In an ideal situation, where scattering particles are spherical with known homogeneous density ρ_s and mean particle radius $\langle a_s\rangle$, and the backscattering behaviour of the particles if well-described through f, SSC can be derived directly from S_v using Equation 5 for each measurement volume. For ADCPs, this applies for every cell or bin in the profile over depth. In practice, information about particle properties is rarely known and usually a varying, heterogeneous mixture of suspended matter such as sand particles, flocculated silt and clay particles, and air bubbles is present in the water column. Therefore, the practical approach to derive SSC from ADCP backscatter in real world applications is to simplify the model to a log-linear relation between S_v and SSC, which must be tuned to site-specific SSC reference measurements using fitting parameters A and B:

$$S_v = A \cdot 10\log_{10}(SSC) + B \quad (6)$$

3 ACCOUNTING FOR PARTICLE SIZE USING MULTI-FREQUENCY BACKSCATTER

3.1 Particle size-acoustic wavelength interactions

As with sensors using OBS, relation (6) should be redetermined whenever monitored particle properties change. Hence, continuous reference measurements must be carried out for recalibration of the backscatter-SSC relation. With the multi-frequency approach, it is proposed to capitalize on the sensitivity of the form function (f) to the emitted signal's frequency due to the interaction between particle size with emitted acoustic wavelength. Through simultaneously monitoring using three different frequencies, the differences between backscatter at those three frequencies can be utilized to infer sediment properties. The Nortek Signature1000 ADCP with three acoustic frequencies on the central beam echosounder of the ADCP ($F = 1000$, $F = 500$, and $F = 250$ kHz) can be used to exploit this sensitivity (Figure 1).

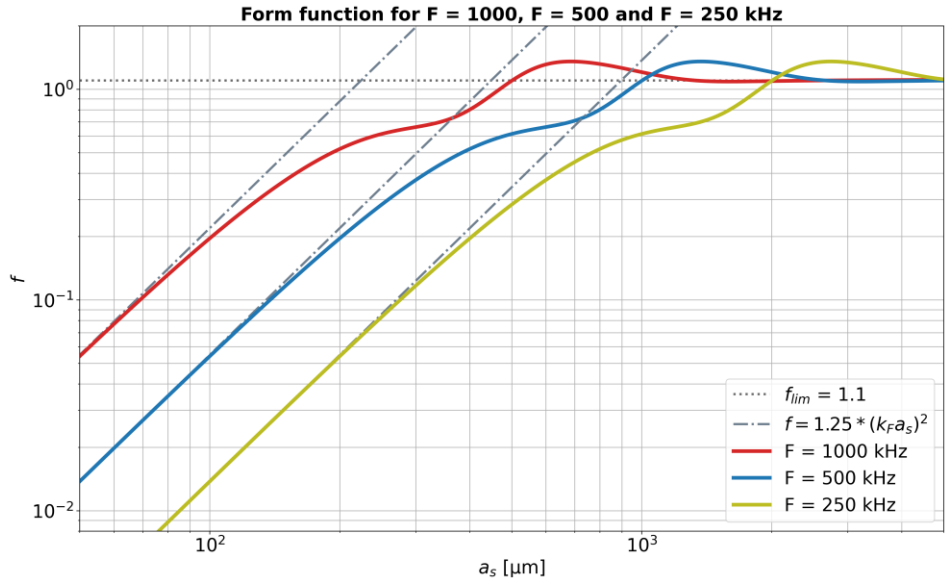

Figure 1. Backscatter form function (f) of quartz sand particles, corresponding to $F = 1000$, $F = 500$ and $F = 250$ kHz. The gray dash-dotted lines indicate the Rayleigh scattering regime, where f is a log-linear relation of the acoustic wavenumber-particle radius product (ka_s). The gray dotted line indicates the geometric regime, where $f = 1.1$ (Thorne & Meral, 2008).

3.2 Acoustic particle radius

By assuming the sediment particle size to be unimodally and narrowly distributed (Jourdin et al., 2014), it is possible to derive an explicit relation between the difference in absolute volume backscatter recorded at two frequencies (ΔS_v) and a theoretical or *acoustic* particle radius (a_s) based on the backscatter form function derived by Thorne & Meral (2008):

$$\Delta S_v = S_{v,1} - S_{v,2} = 10\log_{10}\left(\frac{f_1^2(a_s)}{\langle a_s \rangle} / \frac{f_2^2(a_s)}{\langle a_s \rangle}\right) = 20\log_{10}\left(\frac{f_1(a_s)}{f_2(a_s)}\right) \quad (7)$$

Following this approach, a specific range of particle radii can be estimated as a result of the particle size sensitivity on the frequencies used. For frequencies 1000, 500, and 250 kHz, the resolvable acoustic particle radius range varies for each frequency combination (Figure 2). Using the largest frequency interval available ($F_1 = 1000$ and $F_2 = 250$ kHz), the widest resolvable range is obtained, with an unambiguous solution in the approximate range of $60 \leq a_s \leq 2000$ µm (Figure 2).

3.3 Including acoustic particle radius in the backscatter-SSC model

In contrast to using single frequency ADCPs, where one resorts to Equation 6 in case no additional sediment parameters are measured, deriving acoustic particle radius estimates using a multi-frequency ADCP (Equation 7) allows the use of a backscatter-SSC model that considers particle radius variations. The is referred to as the multi-frequency model:

$$S_v = A \cdot 10\log_{10}(SSC) + 10\log_{10}\left(\frac{f^\beta}{a_s}\right) + B \quad (8)$$

Besides A and B, an additional fitting parameter β is introduced to account for potentially limited applicability of the applied form function (f) on the scattering particles present in the measurement volume. For example, Equation 4 (Thorne & Meral, 2008) was empirically derived for quartz sand particles while in practise clay, silt and organic matter can be present.

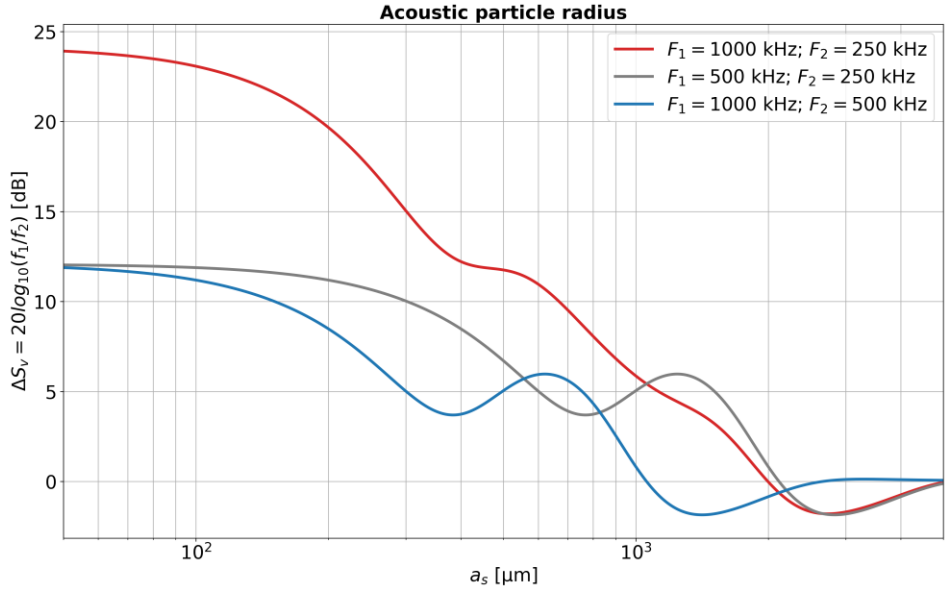

Figure 2. Relation between acoustic particle radius and ΔS_v (Equation 7), based on the quartz sand backscatter form function ratio (f_1/f_2) corresponding to different combinations of $F = 1000$, $F = 500$ and $F = 250$ kHz (Thorne & Meral, 2008).

4 FIELD VALIDATION MEASUREMENTS

4.1 Methods

To assess whether certainty in deriving SSC estimates from ADCP backscatter is improved by considering acoustic particle radius estimates, performance of the single frequency model (Equation 6) and the multi-frequency model considering acoustic particle radii estimates (Equation 8) were compared based on a sample dataset. For this, a field campaign was carried out in Spring 2022 sampling several locations around the island of Texel, The Netherlands (Figure 3). This site was chosen as the type of sediment in suspension differs greatly between the tidal channel connecting the North Sea to the Marsdiep basin (more sandy) and the Marsdiep basin itself (more muddy), and the phase of the tide is expected to affect the sediment type in suspension. Backscatter measurements were taken at frequencies $F1 = 1000$ kHz, $F2 = 500$ kHz and $F3 = 250$ kHz using the central beam echosounder on a Nortek Signature1000 in a vessel mounted (VM) setup. Vertical cell size was set to 0.05 m, a transmit pulse length of 0.1 ms and the default power level (PL) of 0.0 dB was used. Signal pulse compression was not applied.

Simultaneous reference measurements were taken using a Niskin bottle (NB) and a pumping system, where most of the samples were taken in the Molengat (MG) tidal channel using the NB during ebb ($n = 15$) and flood ($n = 2$) (see Figure 3 for sample positions). To exclude effects of inconsistencies in sampling method and to reduce impact of environmental variations between sites, only the NB samples taken at MG were further processed. Based on the assumption that different

types of particles are transported in the tidal channel during different phases of the tide, the dataset was divided into two datasets, where Dataset 1 contained measurements with relatively consistent properties of the suspended particles comprising the ebb samples. Dataset 2 contained ebb and flood samples, representing measurements taken under conditions with varying suspended particle properties. The samples were analysed in the lab for SSC following the procedure mentioned in Jaarsma (2023), taking note of measurement uncertainty (Table 3). No additional particle properties such as particle size were determined.

Figure 3. Various locations were sampled around the Dutch barrier island Texel: Molengat (MG) tidal channel, Marsdiep (MD) tidal inlet, near the Prins Hendrikzanddijk (PHZD) coastal nourishment and Waddenzee (WZ). The North Sea is on the left side of the image, the Waddenzee back barrier basin on the right side.

4.2 Acoustic noise levels and signal intensity

As introduced in Section 2.1, the noise threshold (NT) should be considered and removed before correlating backscatter measurements to SSC (Equation 1). It is good practice to regularly determine NT for each frequency by using the ADCP in 'listening mode', which can be done by setting the power level to -100 dB. Alternatively, noise levels can be estimated by averaging the backscatter intensity recorded in the lowest cells in each profile. Because the ADCP profiling depth was configured to be at least twice the actual water column depth, the last cells in each profile correspond to the signal that has travelled the water column at least twice – first reflecting off the bed and then the water surface (Figure 4). It can be assumed that at this point, the signal has attenuated to an extend where the recorded signal intensity in these cells primarily comprises acoustic noise. NT varied between 20 and 27 dB for the 1000 kHz measurements and between 15.5 and 26.5 dB for 500 kHz measurements, where NT was observed to be largest for the flood measurements.

For the 250 kHz measurements, the signal was above the noise threshold only within a few meters from the instrument and at the sea floor (Figure 4c). Minimal backscatter intensity was recorded over most of the water column which can be attributed to reduced transducer efficiency at this frequency, little presence of particles large enough for sufficient sensitivity at 250 kHz, or a combination of both. Understanding to what extend using the ADCP's central beam echosounder at 250 kHz can be applied in the proposed multi-frequency method requires further assessment in consideration of these remarks. In this study, only the 1000 and 500 kHz measurements were further processed.

4.3 Averaging and calculating volume backscatter (S_v)

The uncorrected backscatter measurements (R_x) taken at 1000 and 500 kHz were aggregated to the water volume sampled using the Niskin bottle based on time and depth of sampling, by averaging over 0.50 m in the vertical domain and 30 seconds in time. The aggregated backscatter was then corrected for noise levels and echosounder loss terms (Equation 1), where the contribution on α attributed to water absorption was estimated following Ainslie & McColm (1998) and attenuation attributed to suspended sediment was neglected.

4.4 Accounting for use of an uncalibrated instrument and narrow frequency interval

Because an uncalibrated instrument was used, no formulation of G (Equation 1) was available leading to an unresolved calibration offset ΔG between the frequencies:

$$\Delta S_v = S'_{v,1000} - S'_{v,500} + \Delta G \tag{9}$$

Here, $S'_{v,1000}$ and $S'_{v,500}$ indicate relative volume backscatter obtained from the 1000 and 500 kHz measurements respectively. To mitigate implications of using an uncalibrated instrument in the multi-frequency approach to infer SSC from ADCP backscatter, the following iteration scheme was applied to estimate the calibration offset between the frequencies (ΔG). By ranging ΔG, Equation 7 was solved for acoustic particle radius based on the varying sets of ΔS_v datapoints that were obtained from Equation 9. These obtained acoustic particle radii were then substituted in the multi-frequency model (Equation 8) and assessed for best fit with the reference SSC measurements, which was found to consolidate to $\Delta G = -31.4$ dB.

Using $F1 = 1000$ kHz and $F2 = 500$ kHz results in unambiguous solutions for a_s when $6.0 < \Delta S_v < 12.0$ dB (blue line in Figure 2). For values of $3.7 < \Delta S_v < 6.0$ dB, multiple solutions for a_s exist, which is a result of the frequency interval being relatively small. Using a larger frequency interval, e.g., $F1 = 1000$ kHz and $F2 = 250$ kHz would result in an unambiguous solution for $0 < \Delta S_v < 24.0$ dB (red line in Figure 2), which was however not possible due to the low backscatter intensities obtained at 250 kHz (Figure 4). For the data points within the ambiguity range, the lowest possible solution for a_s (Table 1) was substituted in the multi-frequency backscatter model (Equation 8). For one of the flood samples it was not possible to derive a_s because ΔS_v was outside the resolvable range (sample 2 in Table 1). Therefore, this sample was removed from the dataset and only one remaining flood sample could be considered in further analysis.

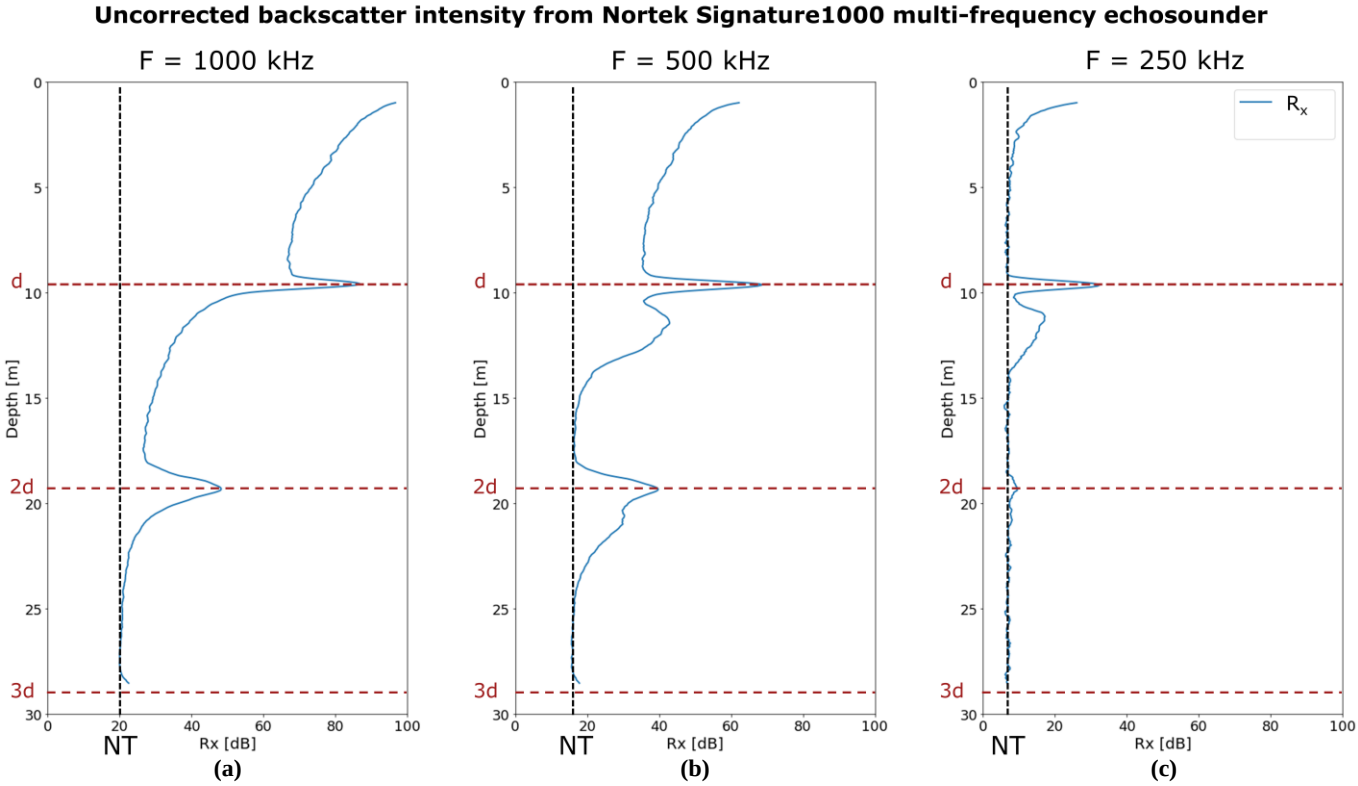

Figure 4. Example profiles of uncorrected backscatter intensity (R_x) at (a) 1000, (b) 500, and (c) 250 kHz recorded simultaneously using the vertical beam echosounder on a Nortek Signature1000 ADCP in the seaward tidal channel MG during flood. The profile depth was configured to be larger than twice the water depth (d, indicated by the red dashed lines). The noise threshold (NT) was estimated based on the uncorrected backscatter intensity recorded in the lowest measurement cells in each profile for all three frequencies.

4.5 Performance of the single vs. multi-frequency approach

The capabilities of using ADCP backscatter to predict SSC is determined by how well the applied backscatter model fits the backscatter measurements based on the reference SSC data. Both the single and multi-frequency backscatter models were applied to Dataset 1 (ebb measurements) and Dataset 2 (ebb and flood measurements), and performance of each fitted relation was assessed based on Pearson correlation coefficients (r^2). Based on the good correlations observed for the single frequency backscatter model (Table 2), this traditional approach is considered suitable for predicting SSC for the ebb only dataset, where the 500 kHz signal ($r^2 = 0.80$) outperformed the default[1] 1000 kHz signal ($r^2 = 0.69$). For the combined ebb and flood dataset, the significantly deviating backscatter intensity recorded for the flood measurement led to a poor fit of the single

[1] By default, the Nortek Signature1000 records backscatter intensity at 1000 kHz using its vertical beam echosounder.

frequency backscatter model (Figure 5a and 5b). Therefore, the single frequency approach is not considered fit to predict SSC under these varying measurement conditions.

The established multi-frequency relations (Equation 8 fitted to $S'_{v,1000}$ and $S'_{v,500}$) are expected to predict SSC well for both datasets based on favorable correlations of the fitted model (Table 2), which is represented in the well aligned backscatter measurements for the combined ebb and flood dataset (Figure 5c and 5d).

The difference in skill to predict SSC between the single and multi-frequency approach is demonstrated by comparing estimates with the SSC reference measurements (SSC_{ref}) (Table 3). The multi-frequency relation with the best fit – Equation 8 fitted to $S'_{v,1000}$ – predicts SSC within the uncertainty range of the reference measurements for 10 of the 16 datapoints, whereas the predictions following the best fitted single frequency relation – Equation 6 fitted to $S'_{v,500}$ – were within the uncertainty range for only 2 of the datapoints (Table 3).

Table 1. Measurements of relative volume backscatter and the absolute difference (ΔS_v, Equation 9) obtained at 1000 and 500 kHz, and corresponding acoustic particle radii (a_s), where a'_s and a''_s represent ambiguous solutions to Equation 7.

Sample	Tide	$S'_{v,1000}$ [dB]	$S'_{v,500}$ [dB]	ΔS_v [dB]	a_s [μm]	a'_s [μm]	a''_s [μm]
1	flood	137.8	94.9	11.5	81	-	-
2	flood	130.5	86.4	12.7	-	-	-
3	ebb	127.4	87.2	8.7	192	-	-
4	ebb	125.4	85.7	8.3	207	-	-
5	ebb	124.6	84.6	8.6	196	-	-
6	ebb	127.9	87.9	8.6	197	-	-
7	ebb	129.6	91.0	7.1	239	-	-
8	ebb	126.4	89.4	5.6	281	549	699
9	ebb	121.8	83.0	7.4	231	-	-
10	ebb	119.8	80.0	8.4	204	-	-
11	ebb	125.0	87.6	6.0	271	-	-
12	ebb	121.0	82.7	6.9	246	-	-
13	ebb	117.8	82.2	4.2	332	447	808
14	ebb	129.9	92.8	5.8	278	564	683
15	ebb	128.1	91.7	5.0	302	496	759
16	ebb	126.2	90.2	4.6	317	470	787
17	ebb	120.4	82.1	6.9	244	-	-

Table 2. Correlation coefficients (r^2) for fitting the single frequency (Equation 6) and multi-frequency (Equation 8) backscatter model to the backscatter measurements for both datasets.

			Single frequency model	Multi-frequency model	
Dataset	n	F	r^2	r^2	β
Ebb	15	1000 kHz	0.69	0.78	-1.0
		500 kHz	0.80	0.80	0.91
Ebb + flood	16	1000 kHz	0.18	0.88	-1.79
		500 kHz	0.41	0.68	-0.45

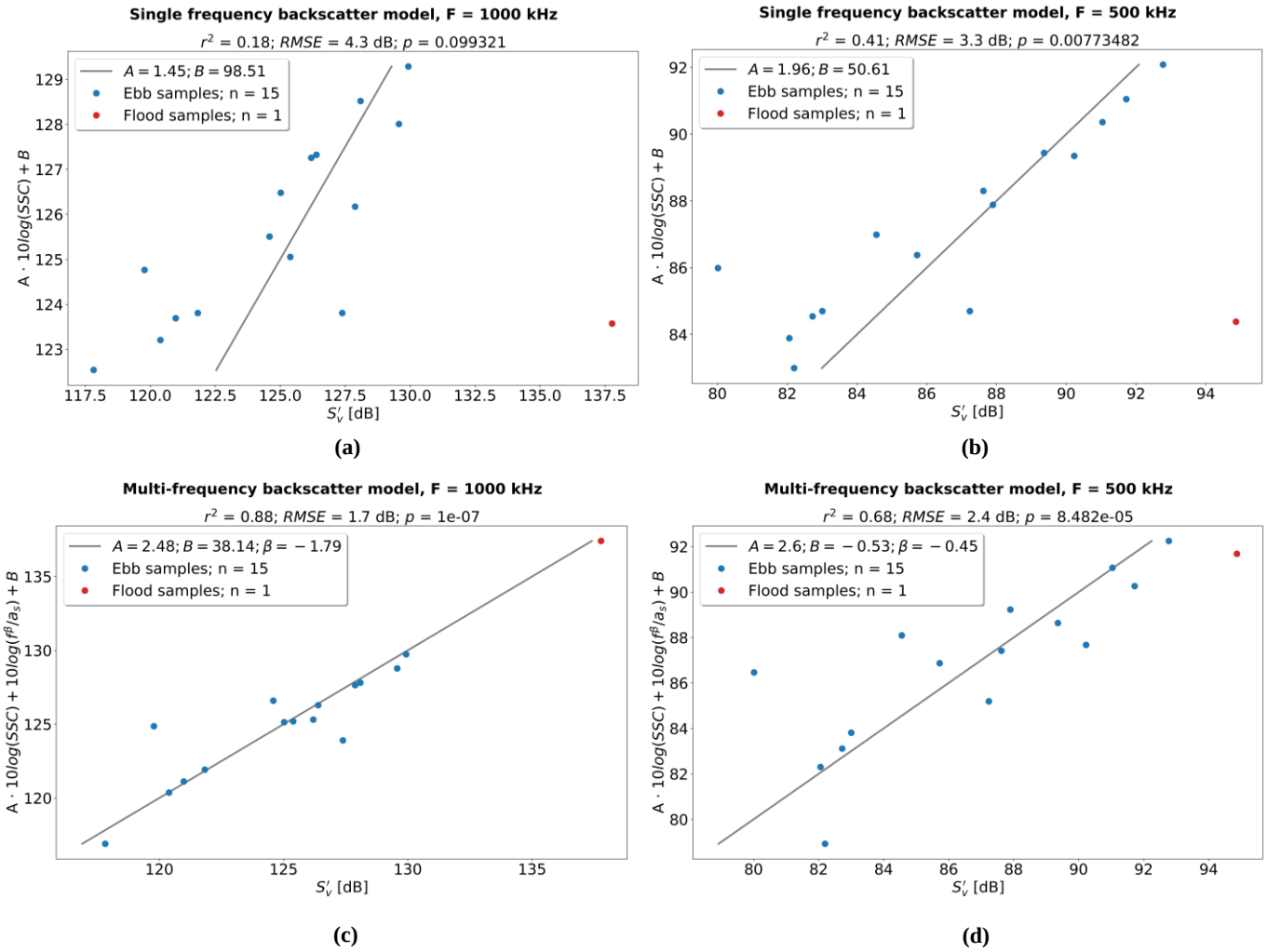

Figure 5. Quality of the single frequency (Equation 6) (a and b) and multi frequency backscatter model (Equation 8) (c and d). Data and linear regression are shown for the 1000 and 500 kHz data based on the combined ebb and flood dataset.

5 DISCUSSION

After establishing a reliable relation with SSC reference measurements, profiles of concentration predictions inferred from ADCP backscatter (Figure 6c) can be combined with flow velocity and direction measurements over the water column (Figure 6a). Based on the findings in Section 4.5, using the multi-frequency approach can make SSC inversions more robust, reducing the need for frequent water sampling to redetermine the backscatter-SSC relation. Because acoustic particle radius can be derived for each measurement cell corresponding to the multi-frequency backscatter signal, it can be plotted over depth together with the flow measurements and SSC predictions (Figure 6b) – leading to potentially valuable information about sediment class. Combining the three measured quantities offers great potential for direct monitoring of sediment transport using a single instrument.

Variations in particle properties have however not been confirmed using a lab analysis, and the size of the sample set leaves room for further investigation on performance of the method. Also, the applied value of β in the fitted multi-frequency backscatter models (Table 2) significantly deviated from the theoretical value of $\beta = 2$ in the general backscatter model (Equation 5), indicating a potentially limited applicability of the applied form function for quartz sand particles (Equation 4) for this sample set.

Table 3. Water sample SSC reference measurements including measurement uncertainty. ADCP backscatter predicted SSC based on the single frequency backscatter model (Equation 6) fitted to the 1000 kHz ($SSC_{SF,1000}$) and 500 kHz signal ($SSC_{SF,500}$) measurements in the combined ebb and flood dataset. Values corresponding to the multi-frequency approach (Equation 8) are also given for the 1000 kHz ($SSC_{MF,1000}$) and 500 kHz ($SSC_{MF,500}$) signal. The marked values correspond to SSC predictions within the uncertainty range of the reference measurements.

Sample	Tide	SSC_{ref} [mg/L]	$SSC_{SF,1000}$ [mg/L]	$SSC_{SF,500}$ [mg/L]	$SSC_{MF,1000}$ [mg/L]	$SSC_{MF,500}$ [mg/L]
1	flood	53 ±3	503	182	55	70
2	flood	59 ±3	-	-	-	-
3	ebb	55 ±3	97	74	76	66
4	ebb	67 ±4	71	62	68	61
5	ebb	72 ±4	62	54	60	53
6	ebb	80 ±3	105	80	82	71
7	ebb	107 ±4	137	115	115	107
8	ebb	96 ±4	83	95	97	102
9	ebb	55 ±3	40	45	55	51
10	ebb	64 ±3	29	32	40	36
11	ebb	84 ±4	67	78	83	86
12	ebb	54 ±3	35	44	53	52
13	ebb	45 ±3	21	41	49	60
14	ebb	131 ±7	145	142	133	137
15	ebb	116 ±7	108	126	119	132
16	ebb	95 ±5	80	105	103	119
17	ebb	50 ±3	32	40	50	49

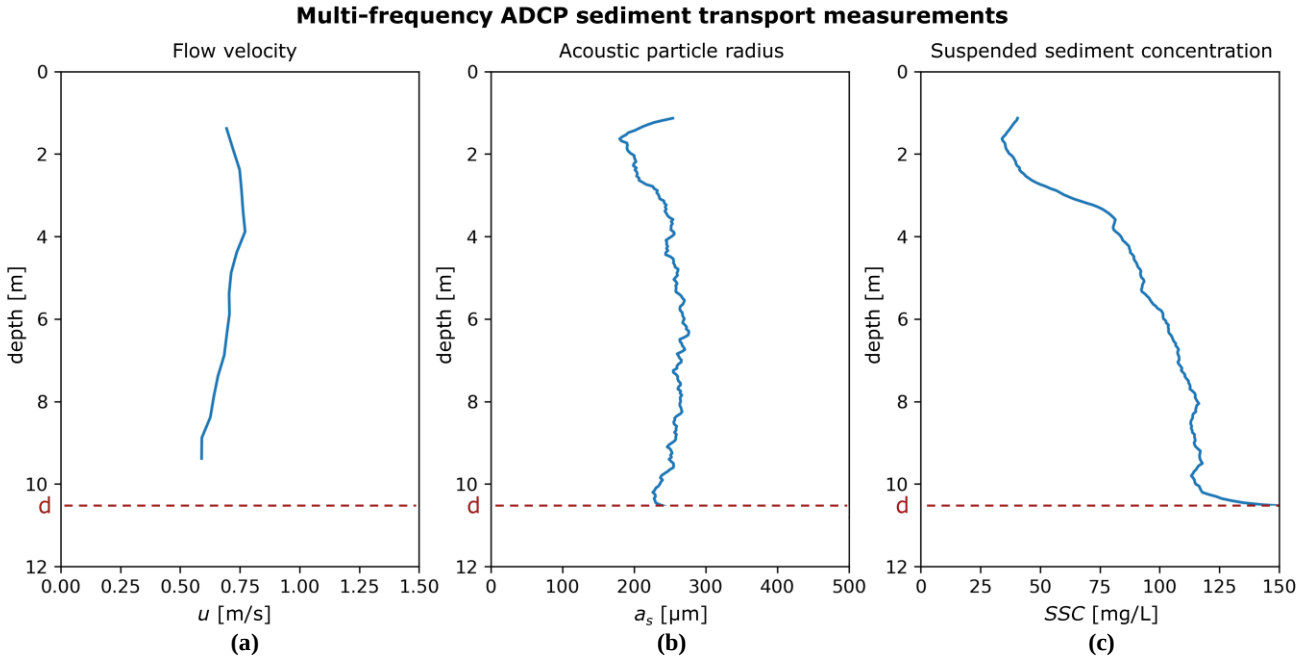

Figure 6. Simultaneous measurements of (a) flow velocity, (b) acoustic particle radius and (c) SSC over depth using the Nortek Signature1000, where *d* indicates the distance between the vertical beam multi-frequency echosounder and the seabed. Because the multi-frequency backscatter measurements are captured using the central, vertical beam echosounder on the ADCP, a higher vertical resolution is obtained and measurements are possible closer to the bed for plots of a_s and SSC compared to the flow velocity measurements.

6 CONCLUSIONS AND RECOMMENDATIONS

For the ebb only dataset, where particle properties were deemed relatively consistent, fitting the traditional single frequency backscatter model (Equation 6) yielded good performance, where a better performance was observed for the 500 kHz signal compared to the default 1000 kHz measurements. For the ebb and flood dataset, very poor correlations were obtained for both frequencies. The observed backscatter corresponding to the sample taken during flood did not align with those taken during ebb, which may have been attributed to the presence of different types of scattering particles in the water column. Following this, the importance of redetermining the relation between backscatter and SSC when scattering properties of particles change, induced by changes in particle size, shape, and nature has been confirmed.

To counteract the sensitivity of established backscatter-SSC relations to changing particle properties, a methodology is proposed where acoustic particle radius (a_s) is derived from multi-frequency backscatter measurements using a Nortek Signature1000 ADCP. By considering these estimates in an adapted form of the backscatter-SSC model (Equation 8), significantly higher correlations between manually sampled and ADCP predicted SSC were obtained for the ebb and flood dataset, aligning the samples taken during each tidal phase.

Applying the multi-frequency method that incorporates acoustic particle radii in the relation between backscatter and SSC on this proof-of-concept dataset shows promising improvement of predicted SSC. Follow-up work should include an analysis of sample's particle diameter to confidently attribute the improved performance of the multi-frequency method to predict SSC under changing sediment properties and should assess a larger sample size. Also, increasing the interval between the two frequencies can overcome solution ambiguity in determining a_s, which could be achieved by investigating methods to increase strength of the 250 kHz signal. Further development of the method can include researching performance in environments with high silt and clay concentrations, considering alternative backscatter form functions and accounting for sediment signal attenuation.

After further validation and development, application of the multi-frequency approach using the vertical beam echosounder on the Nortek Signature1000 ADCP can significantly enhance the capability of predicting SSC and – since backscatter is recorded over depth in conjunction with profiles of current velocity and direction – the ability to monitor suspended sediment transport using a single instrument.

REFERENCES

Acoustics Unpacked. (n.d.). Cornell University. Retrieved 12 January 2024, from http://www2.dnr.cornell.edu/acoustics/AcousticBackground/VolumeBackscatter.html

Ainslie, M. A., & McColm, J. G. (1998). A simplified formula for viscous and chemical absorption in sea water. *The Journal of the Acoustical Society of America*, *103*(3), 1671–1672. https://doi.org/10.1121/1.421258

Demer, D. A., Berger, L., Bernasconi, M., Bethke, E., Boswell, K., Chu, D., Domokos, R., Dunford, A., Fassler, S., Gauthier, S., Hufnagle, L. T., Jech, J. M., Bouffant, N., Lebourges-Dhaussy, A., Lurton, X., Macaulay, G. J., Perrot, Y., Ryan, T., Parker-Stetter, S., … Williamson, N. (2015). Calibration of acoustic instruments. *ICES Cooperative Research Report*, *326*.

Gartner, J. W. (2004). Estimating suspended solids concentrations from backscatter intensity measured by acoustic Doppler current profiler in San Francisco Bay, California. *Marine Geology*, *211*(3), 169–187. https://doi.org/10.1016/j.margeo.2004.07.001

Guerrero, M., & Di Federico, V. (2018). Suspended sediment assessment by combining sound attenuation and backscatter measurements–analytical method and experimental validation. *Advances in Water Resources*, *113*, 167–179.

Guerrero, M., Rüther, N., Szupiany, R., Haun, S., Baranya, S., & Latosinski, F. (2016). The Acoustic Properties of Suspended Sediment in Large Rivers: Consequences on ADCP Methods Applicability. *Water*, *8*(1). https://doi.org/10.3390/w8010013

Guerrero, M., Rüther, N., & Szupiany, R. N. (2012). Laboratory validation of acoustic Doppler current profiler (ADCP) techniques for suspended sediment investigations. *Flow Measurement and Instrumentation*, *23*(1), 40–48. https://doi.org/10.1016/j.flowmeasinst.2011.10.003

Guerrero, M., Szupiany, R. N., & Latosinski, F. (2013). Multi-frequency acoustics for suspended sediment studies: An application in the Parana River. *Journal of Hydraulic Research*, *51*(6), 696–707. https://doi.org/10.1080/00221686.2013.849296

Hay, A. E., & Sheng, J. (1992). Vertical profiles of suspended sand concentration and size from multifrequency acoustic backscatter. *Journal of Geophysical Research*, *97*(C10). https://doi.org/10.1029/92jc01240

Jaarsma, R. A. J. (2023). *Quantifying suspended sediment using multi-frequency echosounder measurements* [Delft University of Technology]. https://repository.tudelft.nl/islandora/object/uuid%3A82cfb0e6-863a-4f85-a8bc-7c5e16c69b05

Jourdin, F., Tessier, C., Le Hir, P., Verney, R., Lunven, M., Loyer, S., Lusven, A., Filipot, J.-F., & Lepesqueur, J. (2014). Dual-frequency ADCPs measuring turbidity. *Geo-Marine Letters*. https://doi.org/10.1007/s00367-014-0366-2

Medwin, H., & Clay, C. S. (1998). *Fundamentals of acoustical oceanography*. Elsevier.

Nauw, J. J., Merckelbach, L. M., Ridderinkhof, H., & van Aken, H. M. (2014). Long-term ferry-based observations of the suspended sediment fluxes through the Marsdiep inlet using acoustic Doppler current profilers. *Journal of Sea Research*, *87*, 17–29. https://doi.org/10.1016/j.seares.2013.11.013

Nortek. (2022). Principles of Operation Signature. *Nortek Manuals*.

Nortek. (2023). *Signature VM Review Manual*. Nortek.

Ocean Illumination. (2021). *Ocean Contour User Guide*.

Plancke, Y. M. G., Vandebroek, E., Claeys, S., & Meire, D. (2017). *Sediment transport in the Schelde-estuary: The challenge of performing good measurements in challenging conditions*. Hydraulic Measurements and Experimental Methods 2017 Conference (HMEM 2017.

Reichel, G., & Nachtnebel, H. P. (1994). Suspended sediment monitoring in a fluvial environment: Advantages and limitations applying an Acoustic Doppler Current Profiler. *Water Research*, *28*(4), 751–761. https://doi.org/10.1016/0043-1354(94)90083-3

Sassi, M. G., Hoitink, A. J. F., & Vermeulen, B. (2012). Impact of sound attenuation by suspended sediment on ADCP backscatter calibrations. *Water Resources Research*, *48*(9). https://doi.org/10.1029/2012WR012008

Thorne, P. D., & Meral, R. (2008). Formulations for the scattering properties of suspended sandy sediments for use in the application of acoustics to sediment transport processes. *Continental Shelf Research*, *28*(2), 309–317. https://doi.org/10.1016/j.csr.2007.08.002

Topping, D., Wright, S., Melis, T., & Rubin, D. (2007). *High-resolution measurements of suspended-sediment concentration and grain size in the Colorado River in Grand Canyon using a multi-frequency acoustic system*. *3*, 19.

Urick, R. J. (1948). The Absorption of Sound in Suspensions of Irregular Particles. *The Journal of the Acoustical Society of America*, *20*(3), 283–289. https://doi.org/10.1121/1.1906373

Urick, R. J. (1983). *Principles of Underwater Sound* (3rd ed.). McGraw-Hill. https://books.google.nl/books?id=hfxQAAAAMAAJ